

EUROPEAN ORGANIZATION FOR NUCLEAR RESEARCH

CERN/LEPC/82-4  
LEPC/I 2  
25.03.1982

Letter of Intent

" O P A L D E T E C T O R "

(An Omn*i* Purpose Apparatus for LEP with  $4\pi$  Coverage)

CERN LIBRARIES, GENEVA



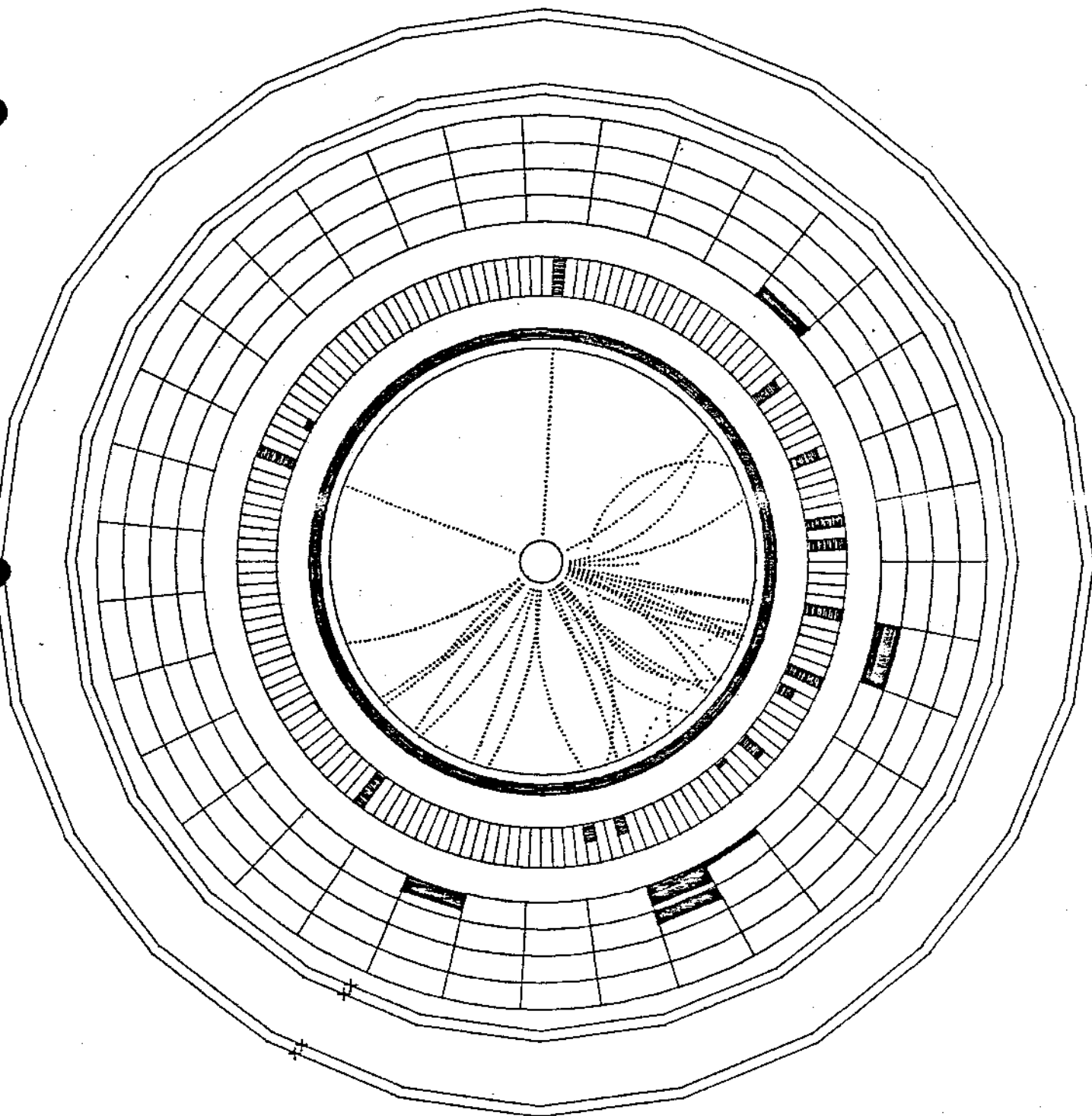
CM-P00043634

LETTER OF INTENT FOR LEP

OPAL COLLABORATION

GEANT-OPAL E+E- ----> HIGGS + E+E- (C.M. ENERGY=100 GEV)

EVENT 2



26 January 1982

LETTER OF INTENT

OPAL-An Omn Purpose Apparatus for LEP with  $4\pi$  coverage

OPAL - COLLABORATION

Birmingham - Bologna - Bonn - Carleton - CERN - Freiburg - Geneva -  
Heidelberg - U.C. London - McGill - Manchester - Maryland - NRCC-Canada -  
Rutherford - CEN Saclay - Tokyo.

- Contents :
- 1) Introduction
  - 2) Physics motivations and their implications for the detector
  - 3) Description of the apparatus
    - 3.1) The central detector
    - 3.2) The superconducting solenoidal magnet
    - 3.3) Time of flight system
    - 3.4) The electromagnetic calorimeter
    - 3.5) The hadron calorimeter
    - 3.6) The muon identifier
    - 3.7) Luminosity monitor and  $2\gamma$  tagging system
    - 3.8) The trigger
    - 3.9) Data acquisition
  - 4) Conclusion
  - 5) Collaborating institutions; cost estimates and responsibilities

## 1) INTRODUCTION

We propose to build a versatile and reliable detector which will be ready for the first operation of LEP. A general purpose detector was chosen because of the wide range of unexplored physics to be studied at the new  $e^+e^-$  machine.

In the energy range accessible at LEP, the mechanisms by which symmetries are broken at present energies should manifest themselves. Among the central physics issues will be the observation of the  $Z^0$  and  $W^\pm$ , the determination of their exact masses and widths, and couplings to leptons and quarks. A general search for new quark flavours, for heavy leptons and for Higgs bosons will be made. These studies as well as searches for more unexpected phenomena such as free quarks and technicolour require a general purpose detector with good energy resolution and particle identification, capable of studying complicated events.

The main components of the proposed detector are the following (fig.1a,b) :

- a) A central detector of the jet chamber type, as in JADE, for efficient tracking of multiparticle events and accurate measurement of particle momenta and  $dE/dx$ .
- b) A superconducting solenoid providing a uniform magnetic field of up to 10 kG.
- c) An electromagnetic calorimeter mounted around the solenoid and covering the full solid angle, consisting of an array of lead glass elements for detection of electrons and photons.
- d) A hadron calorimeter of the iron-scintillator sandwich type for measuring hadronic energy. The iron of the calorimeter will serve as a return yoke for the magnet.
- e) A system of drift chambers for detection and identification of muons over the full solid angle.

The dimensions of the apparatus will be much greater than those of present large solenoidal detectors. However we feel confident of our ability to cope with this technical problem, since the collaboration has specific experience with each of the main parts of the proposed detector.

## 2) PHYSICS MOTIVATIONS AND IMPLICATIONS FOR THE DETECTOR DESIGN

With the advent of LEP we are entering a new, wide range of  $e^+e^-$  energies. Our main motivation is to explore this vast unknown region with an optimum detector. The proposed research programme is an extrapolation of our current knowledge. The most important points, considering the full energy range of LEP, are:

- a) A model independent study of the electromagnetic and weak interactions, when their coupling strengths should become comparable. What are the individual fermion couplings?
- b) If a  $Z^0$  is found, the study of its properties (mass, width and branching ratios). Is the standard model adequate? Are there additional  $Z^0$ 's?
- c) A search for the charged vector bosons  $W^\pm$ , and the study of their decays. A measurement of the triple boson couplings :  $Z^0W^+W^-$  and  $\gamma W^+W^-$ .
- d) The high event rate at the  $Z^0$  peak can be used to study cascade decays of heavy quarks, to look for liberated quarks and to count neutrino flavours.
- e) A search for new particles at the  $Z^0$  peak and elsewhere :
  - i) New fermions such as the top quark, further generations of quarks and leptons and heavy neutral leptons.
  - ii) The neutral Higgs particle ( $H^0$ ) or technipions ( $p^0$ ) through the reactions:  
 $e^+e^- \rightarrow t\bar{t} \rightarrow \gamma H^0(p^0)$  at the toponium peak and  $e^+e^- \rightarrow H^0e^+e^- (\mu^+\mu^-)$  at the  $Z^0$  peak and above.
  - iii) Charged particles, e.g. the charged Higgs ( $H^\pm$ ) or technipions ( $p^\pm$ ) and superpartners of the fermions.
  - iv) Heavy longlived particles.
- f) Precise measurements of the processes  $e^+e^- \rightarrow e^+e^-$ ,  $\mu^+\mu^-$ ,  $\tau^+\tau^-$  and  $e^+e^- \rightarrow$  hadrons at the highest LEP energies, where deviations from current predictions would suggest new phenomena ( $Z'$ , inner structure of fermions etc...).
- g) The investigation of the gauge nature of QCD by studying the triple gluon vertex through the properties of multijet events, by measurement of the energy dependence of  $\alpha_s$ , and by  $\gamma\gamma$  scattering.
- h) A test of grand unification models, through the comparison of the predicted values of  $\sin^2\theta_W$  with those obtained from precise measurements of :
  - i)  $d\sigma/d\Omega$  for  $e^+e^- \rightarrow e^+e^-$ ,  $\mu^+\mu^-$  and  $\tau^+\tau^-$  scanning over the  $Z^0$  peak;
  - ii) the masses of the  $Z^0$  and  $W^\pm$ .

To follow this research programme we have chosen a general purpose detector which can investigate many channels simultaneously. Such a detector is also the best choice for providing sensitivity to unexpected phenomena. The physics aims listed above have some specific implications for the detector :

- Precise studies of electromagnetic and weak interactions (a,b,h) require a  $4\pi$  detector capable of identifying the two-body final states  $e^+e^-$  and  $\mu^+\mu^-$  and measuring their charges down to small angles ( $\theta = 15^\circ$ ) up to the highest LEP energies (f).
- The detector should be capable of identifying energetic electrons and photons from rare processes involving the Higgs and other new particles (e) and of measuring their energy with high precision. This calls for a high resolution electromagnetic shower detector.
- Electron and muon identification over a wide momentum range in multi-hadron final states is necessary, in particular for the study of particles that decay weakly (d,e). (The proposed apparatus can meet these requirements by the combined use of the central detector, the electromagnetic calorimeter and the muon identifier).
- Particle identification (by  $dE/dx$  measurement in our design) will allow the study of decay modes of top particles, Higgs and other new heavy particles (e) and also the search for heavy stable particles such as free quarks (d).
- A segmented  $4\pi$  hadron calorimeter will be needed to detect new charged and neutral leptons (e) by confirming that the missing momentum is not carried by neutral hadrons. It also improves the accuracy in the determination of 2 jet-effective masses resulting from W,Z or Higgs particle decays (c).
- An accurate luminosity monitor will be needed (f) combined with tagging for  $\gamma\gamma$  events (g)
- Abundant statistics are expected in the region of the  $Z^0$  peak; in that case the final precision will be limited by systematic errors. These can be minimized by requiring a stable and uniform detector.

### 3) DESCRIPTION OF THE APPARATUS

In this section we describe the design aims and list the important features of each part of the apparatus, progressing outwards from the interaction region. The general layout of the apparatus is shown in figure 1a,b.

### 3.1 The Central Detector

The central detector consists of 3 parts: a jet chamber, a vertex detector and a z chamber. The jet chamber will record the tracks of charged particles over almost the entire solid angle ( $\Omega/4\pi = 0.96$ ) and measure their momenta. Particle identification will be provided by multiple sampling of the energy loss. The central detector is located inside the solenoid, the visible track length in the (R -  $\phi$ ) plane perpendicular to the beam axis is about 1.6 m, the chamber length is 5 m. These dimensions, together with a value of 5 kG for the magnetic field have been obtained by requiring a momentum resolution  $\sigma_{p_T}/p_T^2$  better than  $2 \cdot 10^{-3}$  (GeV/c) $^{-1}$ , by optimizing particle identification and tracking efficiency and by minimizing the problem of curling tracks. Such a momentum resolution can be reached with a sagitta accuracy of  $\sigma_s = 80 \mu\text{m}$ , which is compatible with our present experience.

With this resolution charge identification for particles with  $p = 150 \text{ GeV}/c$  becomes possible at angles down to  $\theta = 15^\circ$  with respect to the beam axis, corresponding to a solid angle acceptance  $\Omega/4\pi = 0.96$ . The resolution in  $dE/dx$  depends on the effective track length, the number of samplings, and the control of systematic errors. We expect to achieve a resolution of  $\sigma_{dE/dx} = (3-4)\% \cdot dE/dx$ .

This performance can be achieved with a jet chamber. In such a chamber a large number of space points is recorded on each track thereby providing good momentum measurement,  $dE/dx$  information and efficient tracking of multiparticle events. The chamber design proposed here is based on the experience gained with the central detector of the JADE experiment but it incorporates significant technical improvements. The gas used there (4 atm argon with 10% hydrocarbons) would provide the space resolution and particle identification we aim at. Alternative solutions with lower pressure are under study. It is planned to use the beam pipe and the inner wall of the cryostat as parts of the pressure vessel.

The jet chamber consists of 24 segments (Fig.2a), each containing a single wire plane of 160 sense wires alternating with potential wires. This arrangement is chosen in order to minimize systematic errors and facilitate pattern recognition. It is also well matched to the radial distribution of machine induced background (short drift length in regions of high background rates).

The anode and cathode planes have to be supported in such a way that the systematic error in track positioning is below 50  $\mu\text{m}$ . The design study carried out so far has resulted in a viable solution. A system of laser beams or alternatively of X-ray beams will be used to calibrate the chamber with straight tracks. We note that at JADE, a systematic error on the sagitta of  $\sigma_s = 100 \mu\text{m}$  has been reached even without such a calibration system.

For the read-out electronics (which records drift times and signal charges with multiple hit capability) we are studying a new system based on 100 MHz flash-ADC's, to allow pulse shape analysis. A prototype has already been constructed. Its test with a drift chamber gave encouraging results. We found a space resolution (random error per hit) of  $\sim 100 \mu\text{m}$ , essentially independent of the drift path, a satisfactory accuracy in the determination of the signal charge, and an excellent double track resolution ( $\approx 2 \text{ mm}$ ). This random error together with an estimated systematic error of 50  $\mu\text{m}$  is fully adequate to achieve the design goal.

Fig.2b shows the separation of hadrons and electrons through measurement of  $dE/dx$ , based on a resolution of 3.5% r.m.s. for an effective track length of 1.3 m. This resolution is an extrapolation of measurements made with a pressurized test chamber. One can see that particle identification will be possible in the region of relativistic rise as well as at lower momenta. The identification of fractionally charged particles will be very efficient.

The z-coordinates are measured in the jet chamber by charge division with an accuracy  $\sigma_z = 0.5\%$  of the wire length, corresponding to an error of a few milliradians on the track direction. Special z chambers will be used in order to obtain a more precise measurement of the z coordinate at the outer circumference (0.5 mm r.m.s.). These chambers have azimuthally stretched wires and are mounted inside the mechanical support of the jet-chamber (fig.2a). They will significantly improve the mass resolution at low masses (we expect  $\sigma_m = 1-5 \text{ MeV}/c^2$  for  $K^0$  and  $\Lambda^0$ ). Another accurate measurement of z will be performed in a vertex chamber close to the beam pipe.



The vertex chamber will be located between the beampipe and the jet chamber and will be capable of measuring both  $(R, \phi)$  and  $z$  coordinates with increased precision. Its main purpose will be the identification of decay vertices of short lived particles. The details of this chamber (and its possible performance) are under study.

### 3.2 The superconducting solenoidal magnet (Fig.3a,b)

The magnet consists of a superconducting solenoid 4 m in diameter and 6.6 m in length, surrounded by an iron yoke composed of a barrel and two endcaps. It is designed for a homogeneous magnetic field of up to 10 kG<sup>\*)</sup>. The total thickness of the solenoid, including the cryostat is  $\sim 12$  cm of aluminium, or  $\sim 1.5$  r.l.. In the cylindrical gap between the solenoid and the yoke barrel the magnetic field has to be low, as required by the operation of the photomultiplier tubes (pms) of the lead glass calorimeter. For this purpose two small conventional compensating coils located at the two ends of the solenoid might be used.

The yoke is made of laminated iron plates 5 to 10 cm thick, separated by about 10 mm to provide space for the scintillator sheets of the hadron calorimeter, and weighs approximately 2000 tons. It is divided into two independent half yokes (left and right) (Fig.3b), each containing half of the iron barrel and the corresponding half of each endcap. Each half yoke is mounted on an independent mobile platform. Before removing one of the two half yokes, the corresponding half endcaps have to be extracted axially by approximately 1.5 m with respect to their normal position (Fig.3a).

When the yoke is separated from the solenoid, adequate access becomes available to the central detector and to the barrel lead glass calorimeter, without the need to break the beam pipe vacuum. The solenoid with the central detector and the lead glass barrel are mounted on a single support structure. Mobile platforms enable the assembled magnet and detector to be moved between the garage and the beam position.

---

\*) Although 5 kG is the preferred field for normal operation we believe that the additional cost resulting from the selection of a solenoid design capable of 10 kG is justified by the increased flexibility this gives.

### 3.3 The Time of Flight System

The purpose of the TOF system is to provide triggering information, to reinforce the identification of  $\pi^{\pm}$ ,  $K^{\pm}$  and  $p$ ,  $\bar{p}$  at low momenta and to identify cosmic ray muons. It consists of a barrel and two endcap sections.

The barrel (Fig.1a) is made from bars of scintillator each 6 m long, 8 cm wide and 3 cm thick, located near the outer surface of the cryostat. The time resolution will be of the order of  $\sigma_{\text{TOF}} = 250$  psec over a flight path of at least 2 m. Each endcap section is made of 24 elements which correspond to the sectors of the central detector.

### 3.4 The Electromagnetic Calorimeter

The electromagnetic calorimeter is composed of a barrel which covers 80% of the solid angle and two endcaps which cover the remainder. The total acceptance of the barrel and the two endcaps is 97% of  $4\pi$ . It will measure the energy and direction of photons and electrons. Excellent energy resolution is very important, in particular for detecting high energy electrons and photons accompanying Higgs particles. We also aim at high hadron rejection and good two shower separation.

For these reasons (and also taking into consideration reliability and ease of operation) we have chosen a system of lead glass Cerenkov counters. In addition a presampling device in front of the barrel detector will improve particle identification and energy resolution.

The barrel is situated between the coil (1.5 r.l. of aluminium thick) and the iron return yoke of the solenoid. It contains about 11000 closely packed wedge shaped blocks of SF6 glass arranged in about 130 modular half rings of 80 counters. The blocks are 21.4 r.l. deep with a cross section of  $\sim 100 \times 100$  mm<sup>2</sup> at the back face, on which is mounted a 3" photomultiplier (pm). The requirement of low field in the region of the barrel calorimeter is specifically taken into account in the design of the magnet (see section 3.2). Each block will be calibrated in an electron beam before installation. The pm gains will be monitored with a system of flash lamps and optical fibres. While running, a continuous calibration will be possible with electrons of known energy.

We have recently performed tests with arrays of such counters. The energy resolution is described by the formula :

$$\sigma_E/E = 4\%/\sqrt{E} + 0.1\% [E \text{ in GeV}]$$

up to 100 GeV (Fig.4a) (The coil will modify  $\sigma_E/E$  below 5 GeV). The measured uniformity of each array is better than 0.5%. A hadron rejection factor of 200 at 5 GeV rising to 600 at 50 GeV has been obtained with 95% electron detection efficiency (Fig.4b). The average spatial resolution, obtained from the sharing of energy between blocks, is 4 mm r.m.s. for 40 GeV electrons; this is independent of the angle of incidence. Monte Carlo simulations suggest that the granularity provided by 11000 blocks is sufficient to study new processes such as those discussed in section 2. A detailed simulation also indicates that the electrons in narrow jets can be identified by combining the  $dE/dx$  information from the jet chamber with the shower energy information. The resulting overall hadron rejection is estimated to be better than  $10^{-4}$ .

The presampling device uses the coil as a converter. It consists of multiwire proportional chambers, with helical cathode strips, equipped with ADCs. It also makes use of the pulse height measurement in the TOF counters. Its functions are a) to improve the single photon to  $\pi^0$  separation, b) to improve electron to hadron discrimination and c) to correct for the energy loss of photons and electrons in the 1.5 radiation lengths of the coil, thus maintaining good energy resolution down to low energies.

Each of the proposed endcap calorimeters consists of 1500 blocks of lead glass, 21.4 r.l. deep, with a square cross section of 85 x 85 mm<sup>2</sup>. The blocks cannot be viewed with conventional pms, since they are located in a region where the magnetic field can be as high as 10 kG (at full solenoid current). Our present intention is to use vacuum photodiodes or single stage pms equipped with high gain, low noise, integrated circuit amplifiers. The orientation of the magnetic field at the endcaps is particularly favourable for this scheme. Prototype devices are currently being tested. If these investigations do not prove the feasibility of this approach we will either construct liquid argon detectors or adopt a lead scintillator BBQ scheme. Preliminary investigations indicate that both of these solutions are feasible; however our choice is to use the powerful lead glass technique over the full solid angle.

### 3.5 The Hadron Calorimeter

A hadron calorimeter with uniform  $4\pi$  coverage is necessary in order to trace the total energy flow event by event. The proposed design allows for example the separation of events with undetected neutrinos as expected from heavy lepton production from events with neutral hadrons, the study of

hadron jets and the reconstruction of  $e^+e^- \rightarrow W^+W^- \rightarrow 4$  jets. It also provides a total energy measurement needed for a bias free study of multihadrons by discriminating against  $\gamma\gamma$  events.

It is a natural technical solution to calorimetrize the iron yoke of the magnet. As foreseen at present this will be done by sandwiching iron sheets with scintillator. The calorimeter consists of a barrel and two endcaps.

The barrel is composed of 26 modules (Fig.1a,b), 8 m long, each made of 16 steel plates, 50 mm thick and separated by 10 mm. The light from the scintillators, sandwiched between the steel plates, is collected by thin BBQ wave shifter sheets, placed between the barrel modules. The read out is grouped into about 1000 (radial) towers, each = 50 x 50 cm<sup>2</sup> in cross section and viewed by one pm per tower. Results from preliminary tests of a full size prototype of the proposed calorimeter with lead glass in front indicate an energy resolution of the order of 80%/√E.

The endcap, similar to the barrel in its basic sandwich structure, has a different iron segmentation because of the design of the magnet poles. We are studying technical solutions for efficient light collection by BBQ rods traversing the full thickness of the poles.

The optimization of the hadron calorimeter design depends on the final design of the magnet and on further tests on combining lead glass and hadron calorimeter information.

An alternative technique using gaseous detectors for the hadron calorimeter is under study. It will be considerably cheaper than the solution with scintillators. Tests on a prototype are in preparation.

### 3.6 The Muon Identifier

Measurements on exclusive muon pairs will give direct information on electroweak theories. Properties of heavy quarks (b,t,..) can be studied through muons produced in semi-leptonic decays, including multiple muons from cascades of such decays (e.g.  $t \rightarrow b + c + s$ ). Thus there is interest in pairs of muons with the full beam energy, and also single and multiple muons (with accompanying hadrons) with energies down to a few GeV. Good coverage of the full solid angle is necessary, particularly to get good data on the inclusive multimMuon processes.

Muons will be identified by their penetration through the lead glass and iron (6 absorption lengths). The probability for a 10 GeV pion to penetrate this amount of material has been measured to be about 0.5% (tests by UAl group). It should be possible to identify direct muons of momentum greater than 2-3 GeV/c.

The cylindrical part of the experiment will be covered by four layers of drift chambers 4.6 m from the beam, covering 70% of  $4\pi$ . Each chamber will be 60 cm wide with a single anode wire 9.5 m long. The longitudinal coordinate will be measured by time difference. If necessary a different geometrical arrangement could be used to improve it; the final design will depend on experimental tests and Monte Carlo simulation.

A small amount of absorber will be placed between the layers to minimize background from low energy particles in hadronic showers and from synchrotron radiation. The geometry is designed to optimize the matching of muon tracks to the well defined tracks in the inner detector. A resolution of a few mm in the  $(R, \phi)$  plane will be adequate from consideration of multiple scattering.

The remainder of the apparatus will be covered at each end by up to 8 square planes of drift chambers (4 with vertical wires, 4 with horizontal wires), because good measurement in both transverse coordinates is necessary to match the inner detector in this case. This completes almost  $4\pi$  coverage for the identification of muons.

### 3.7 Luminosity Monitor and $2\gamma$ Tagging System

The luminosity monitor will measure Bhabha scattering at small angles where weak interaction effects are negligible. It will also tag events coming from the exchange of two photons. The monitor-tagger (Fig.1a) covers the angular interval between 30 and 110 milliradians relative to the beams. The elements comprising each of these monitors (proceeding outward from the interaction point) are listed below :

- a) Two pairs of multiwire proportional chambers spaced 20 cm apart for tracking particles.

- b) Four precisely located scintillation counter pairs with restricted but precise solid angle coverage to provide a precision luminosity monitor. The Bhabha rate through these counters will be a few events per second at the full LEP design luminosity.
- c) A pre-radiator of two radiation lengths of lead, followed by scintillator. (This might be replaced by BGO).
- d) A further multiwire proportional chamber, to help in accurate position determination for photon initiated showers.
- e) A forward E.M. calorimeter which consists of a lead-scintillator sandwich of 28 r.l.. The light will be collected by BBQ strips and long light guides to external photomultipliers. We are investigating the alternative of using vacuum photodiodes located before the quadrupoles instead of piping the light out.

In addition there will be a drift chamber of 1 m diameter in front of each electromagnetic endcap calorimeter.

### 3.8 The Trigger

The trigger will be flexible and will combine information from the different detector components. The following trigger elements are foreseen :

- a) The fast scintillator-trigger requires suitable combinations of TOF counters.
- b) The energy-trigger requires energy deposited in the electromagnetic shower detector and/or in the hadron calorimeter.
- c) The track-trigger asks for a certain number of tracks in the central detector.
- d) The tagging-trigger requires shower energy in the forward detector.
- e) The quark-trigger, uses a real time measurement of energy loss of charged particles in the Central Detector. It is intended to be sensitive to particles of charge  $(1/3)e$ .
- f) The muon-trigger requires penetrating tracks in the muon chambers.

By suitable combinations of these trigger elements we can fulfill the requirements corresponding to the proposed physics programme.

### 3.9 Data Acquisition

The data acquisition system will be based on intelligent interfaces placed between the detectors and the data acquisition computer.

Data are first collected by fast programmable processors which perform data correction and compacting. The second level of the data acquisition system consists of a set of autonomous branches corresponding to the

different parts of the detector. Each branch is controlled by an intelligent branch driver which performs further data reduction and analysis and transfers data to local (branch) buffer memories.

A minicomputer system collects data from the buffer memories and performs final monitoring and experimental control. This computer will also provide the support of the microprocessor network within the acquisition system.

With this scheme each part of the detector can be set up, calibrated, tested and monitored independently. We envisage having a powerful off line computer near the experiment in view of the expected high data rates and event complexity.

#### 4) CONCLUSION

The proposed detector is capable of detecting charged and neutral particles over essentially the full solid angle surrounding an intersection of LEP. It has the following features (see Table 1) :

- i) Measurement of the momenta of charged particles with high resolution.
- ii) Identification of particles by ionization and time of flight measurements.
- iii) Identification and measurement of photons and electrons in a fine grained detector, with excellent energy resolution.
- iv) Measurement of the energies of charged and neutral hadrons in a segmented calorimeter.
- v) Identification of muons from a few GeV to the highest energy.

This detector will certainly allow all the investigations mentioned in section 2 to be made. The good energy resolution and full coverage for all particles is essential for the separation of single virtual photon and  $Z^0$  processes from two-photon events. Measurements of charge asymmetries of lepton states up to the full energy can be carried out down to  $15^\circ$ . High energy photons, such as are expected in association with Higgs particles, can be measured with excellent resolution. The electrons and muons expected from the decay of heavy flavours can be identified and measured accurately. The forward electron detectors tag two-photon events.

The wide variety of precision experiments possible with the proposed detector demonstrates its versatility. The main characteristics of the detector are essential for the experiments to be performed in the new range of LEP energy.

While the detector contains a number of novel features - not least, its size - it is soundly based on proven techniques. We are sure that its construction is well matched to the experience and technical expertise of the collaboration.

TABLE 1 - Summary of the major components of the experiment

<u>Component</u>	<u>Description</u>	<u>Main Parameters</u>
Magnet	Superconducting solenoid with iron return yoke	Field volume 6.6m long x 4m diameter Maximum field 10 kG Coil thickness 1.5 r.l.
Central Detector	"jet" type drift chamber (+ high resolution vertex chamber + z chamber)	Solid angle = $0.96 \times (4\pi)$ Visible track length 1.6m $\sigma_{P_T} / p^2 = \pm 1.5 \times 10^{-3} \cdot [\text{GeV}/c]^{-1}$ $\sigma(\text{sagitta}) = \pm 80 \mu\text{m}$ $\sigma(dE/dx) = 3.5 \times 10^{-2} \cdot dE/dx$ $\sigma_{\theta}(\text{jet chamber}) = 4 \text{ mrad}$ $\sigma_{\theta}(\text{vertex} + \text{z chamber}) = 0.3 \text{ mrad}$
EM Calorimeter	SF6 Lead Glass (barrel $\sim 10^9$ blocks, endcaps $\sim 3 \times 10^8$ blocks)	Solid angle = $0.97 \times (4\pi)$ Depth 21.4 r.l. $\sigma_E/E = \pm(4/\sqrt{E} + 0.1)\% [E \text{ in GeV}]$ $\sigma(\text{position}) = \pm 4\text{mm} (40 \text{ GeV } e^-)$
Hadron Calorimeter	Iron-scintillator tower structure ( $\sim 50 \times 50 \text{ cm}^2$ )	Depth 4.7 absorption lengths $\sigma_E/E = \pm 80/\sqrt{E} \% [E \text{ in GeV}]$
Muon Detector	Drift chambers	Absorber = 6 absorption lengths
TOF-System	Scintillator hodoscope	$\sigma_{\text{TOF}} = 250 \text{ psec}$
Forward Detector	Luminosity monitor, small angle tagger	$\sigma_E/E = \pm(17/\sqrt{E})\% [E \text{ in GeV}]$ 30-110 mrad angular coverage

5) COLLABORATING INSTITUTIONS, COST ESTIMATES AND RESPONSIBILITIES

Table 2 gives the list of all the institutions from which physicists and engineers have taken part in the work for the preparation of this letter of intent. Also indicated is the name of a person representing each institution for the purpose of this letter of intent.



TABLE 2

Dept. of Physics, University of Birmingham; UK	[T. McMahon]
Istituto di Fisica and INFN, Università di Bologna; I	[G. Giacomelli]
Physikalisches Institut, Universität Bonn; D	[G. Knop]
European Organization for Nuclear Research, Geneva; CH	[A. Michelini]
Fakultät für Physik, Universität Freiburg; D	[K. Runge]
DPNC, Université de Genève; CH	[P. Extermann]
Physikalisches Institut, Universität Heidelberg; D	[J. Heintze]
Dept. of Physics, The University of Manchester; UK	[P. Murphy]
Dept. of Physics and Astronomy, Univ. of Maryland (CP); USA	[G. Zorn]
Rutherford Appleton Lab, Chilton; UK	[R.M. Brown]
DPHPE, CEN Saclay; F	[P. Le Dû]
LICEPP, Dept. of Phys., Faculty of Science, Univ. of Tokyo; J	[M. Koshiwa]
Dept. of Physics and Astronomy, Univ. College, London; UK	[D.J. Miller]
NRCC + Dept. of Physics, Carleton Univ., Ottawa	[C.K. Hargrove]
IPP + Dept. of Physics, McGill Univ., Montreal; CAN	

Table 3 summarizes the present cost estimate of the detector in 1981 prices.

TABLE 3

<u>DETECTOR</u>	<u>COST (MSF)</u>
Central detector	11.0
Beam pipe	0.5
Magnet :	
Superconducting solenoid	4.5
Cooling system	2.0
Mobile platform	2.0
Fe-yoke	7.5
T.O.F. hodoscope	0.8
E.M. barrel calorimeter	15.0
E.M. barrel presampling	1.0
E.M. endcap calorimeter	4.0
Hadron calorimeter	5.0
Muon detector	4.0
Forward detector (Luminosity monitor, 2 $\gamma$ tagging with tracking chambers)	1.4
Trigger system	1.0
Data acquisition system	2.5
Installation	<u>1.0</u>
<u>TOTAL</u>	<u>63.2</u>

Table 4 gives a possible sharing of responsibilities among the institutions of the collaboration.

TABLE 4

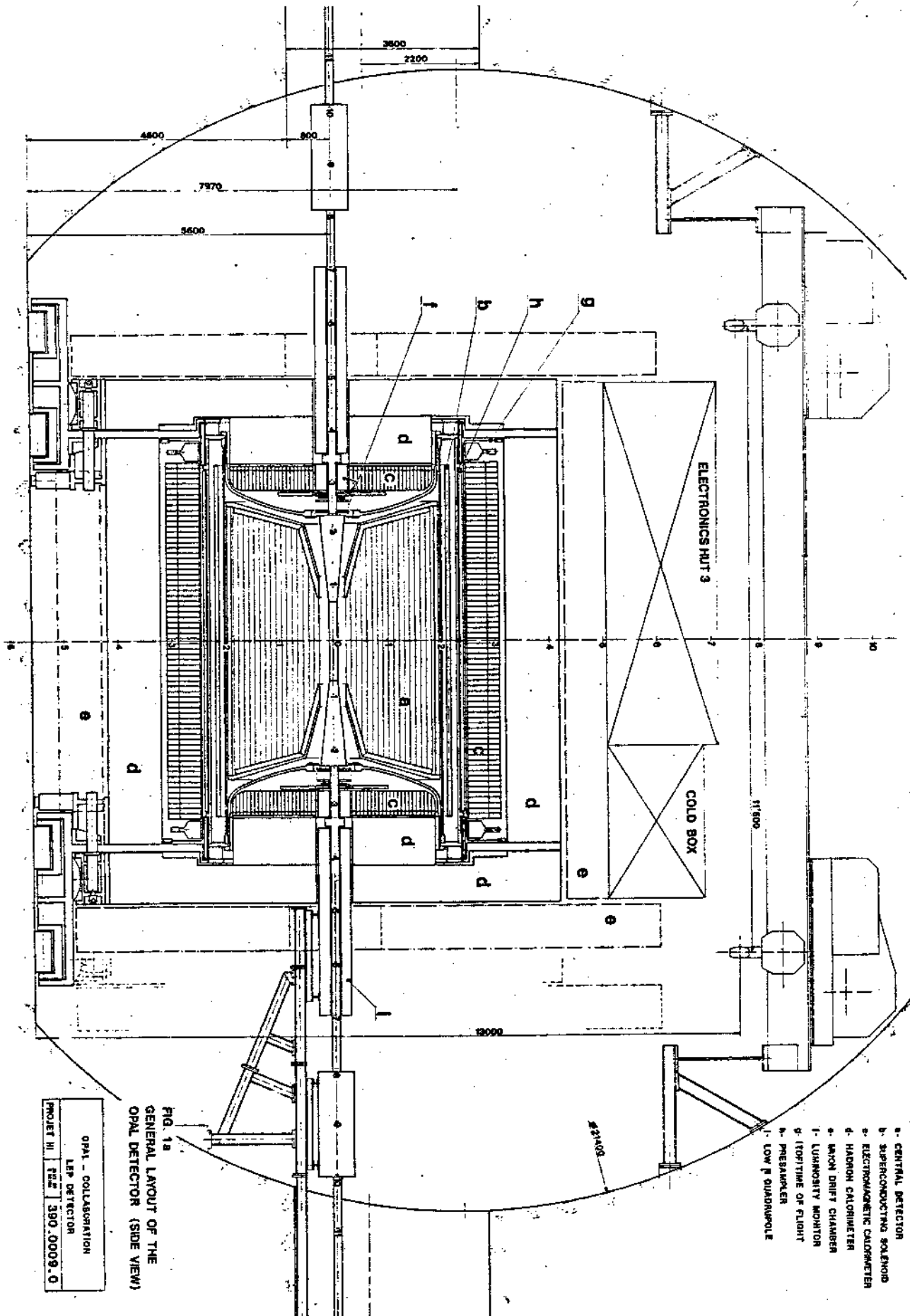
<u>INSTITUTIONS</u>	<u>MAIN RESPONSIBILITIES</u>
Birmingham + Manchester + RAL + University College	E.M. endcap, Muon detector, Data acquisition, Trigger system, Forward detector
Bologna + Maryland	Forward detector, Data acquisition
Bonn + Freiburg + Heidelberg	Central detector, Data acquisition
Carleton + McGill + NRCC-Canada	Vertex detector, Data acquisition, Hadron calorimeter
CERN	Magnet, Hadron calorimeter, Central detector pressure vessel and gas system, Beam pipe
Genève	E.M. barrel presampling detector
Saclay	Data acquisition, TOF hodoscope, Trigger system
Tokyo	E.M. barrel calorimeter, Central detector, Trigger system

Table 5 indicates an estimate of the financial contribution to the detector from each institution.

TABLE 5

<u>INSTITUTIONS</u>	<u>CONTRIBUTION (MSF)</u>
Birmingham + Manchester + RAL + University College	10.0
Bologna	0.7
Bonn + Freiburg + Heidelberg	8.0
Carleton + McGill + NRCC-Canada	6.0
CERN	13.0
Genève	1.0
Maryland	1.3
Saclay	3.0
Tokyo	<u>20.0</u>
TOTAL	<u>63.0</u>

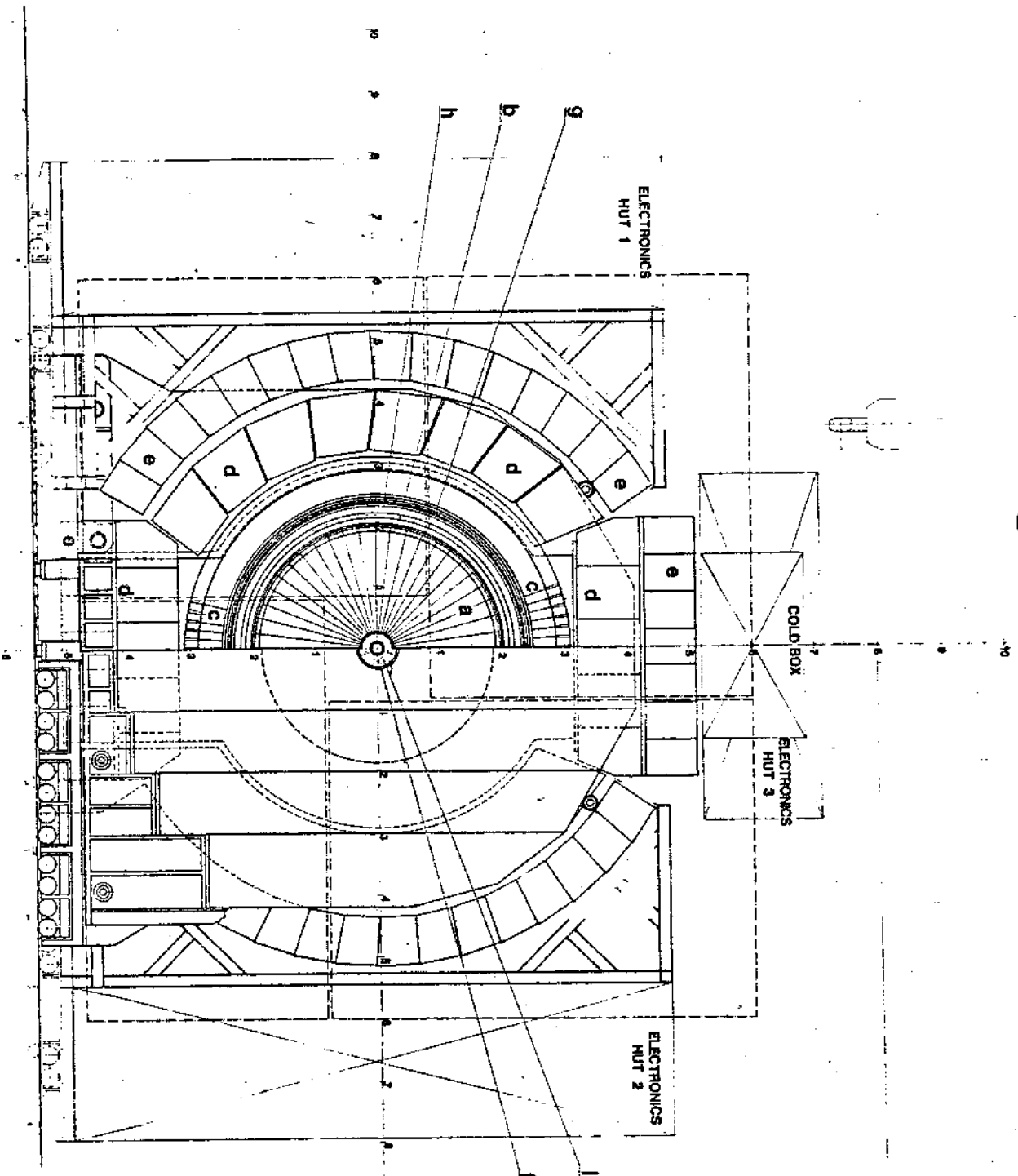
Comparison of Table 5 to Table 3 shows that the financial resources approximately match the estimated cost of the detector.



- a. CENTRAL DETECTOR
- b. SUPERCONDUCTING SOLENOID
- c. ELECTROMAGNETIC CALORIMETER
- d. HADRON CALORIMETER
- e. NEUTRON DRIFT CHAMBER
- f. LUMINOSITY MONITOR
- g. (TOP) TIME OF FLIGHT
- h. PRESAMPLER
- i. LOW P QUADRUPOLE

FIG. 1a  
 GENERAL LAYOUT OF THE  
 OPAL DETECTOR (SIDE VIEW)

OPAL - COLLABORATION  
 LEP DETECTOR  
 PROJECT III FILE 390.0009.0



- a- CENTRAL DETECTOR
- b- SUPERCONDUCTING SOLENOID
- c- ELECTROMAGNETIC CALORIMETER
- d- HADRON CALORIMETER
- e- MUON DRIFT CHAMBER
- f- LUMINOUSITY MONITOR
- g- TIME-OF-FLIGHT
- h- PRESAMPLER
- 1- LOW P QUADRUPOLE

FIG. 1b  
GENERAL LAYOUT OF THE  
OPAL DETECTOR (END VIEW)

OPAL - COLLABORATION	
LEP DETECTOR	
PROJECT N°	390.0010.0

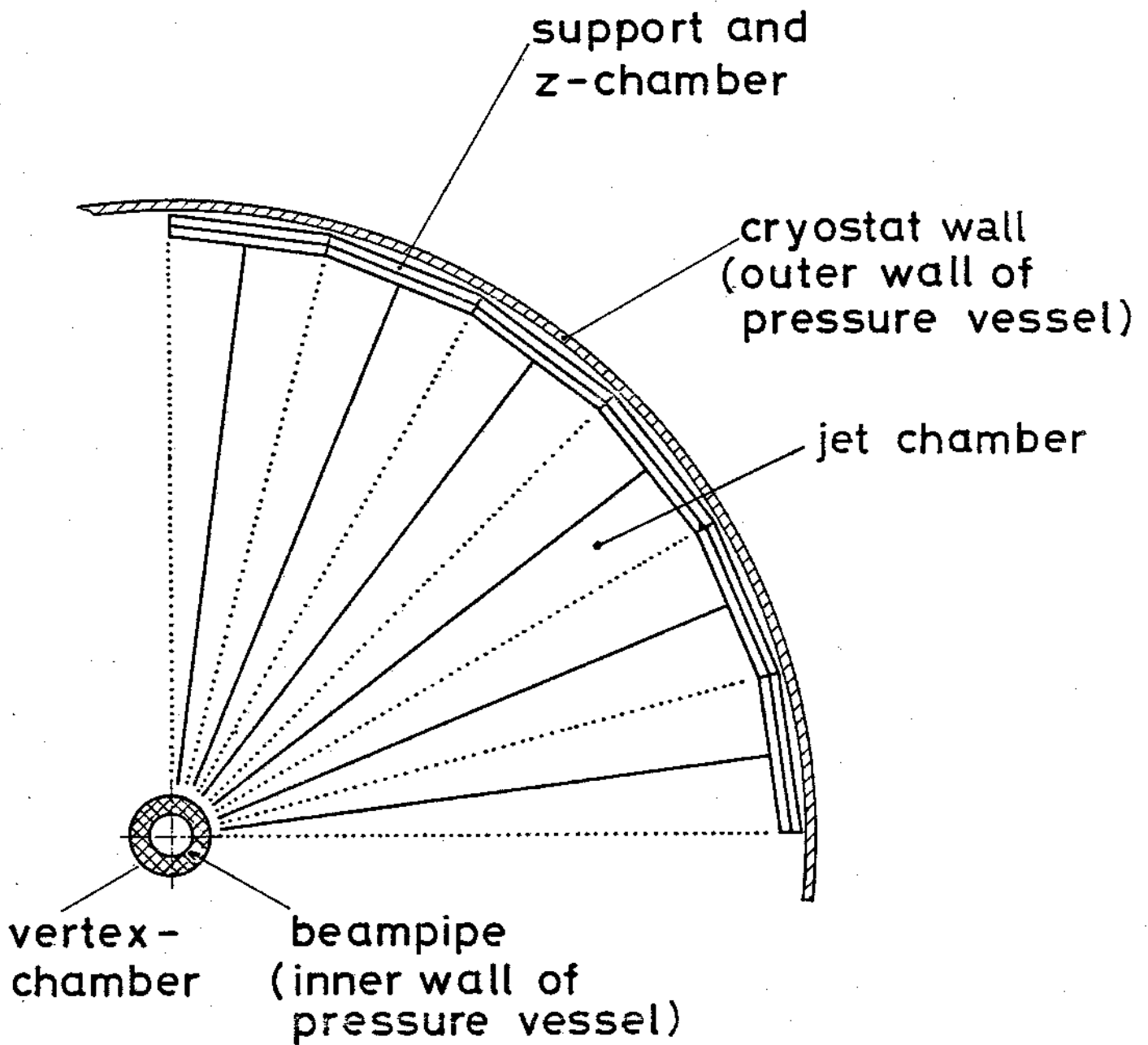


FIG. 2a

Quadrant of Central  
Detector, schematic  
cross section

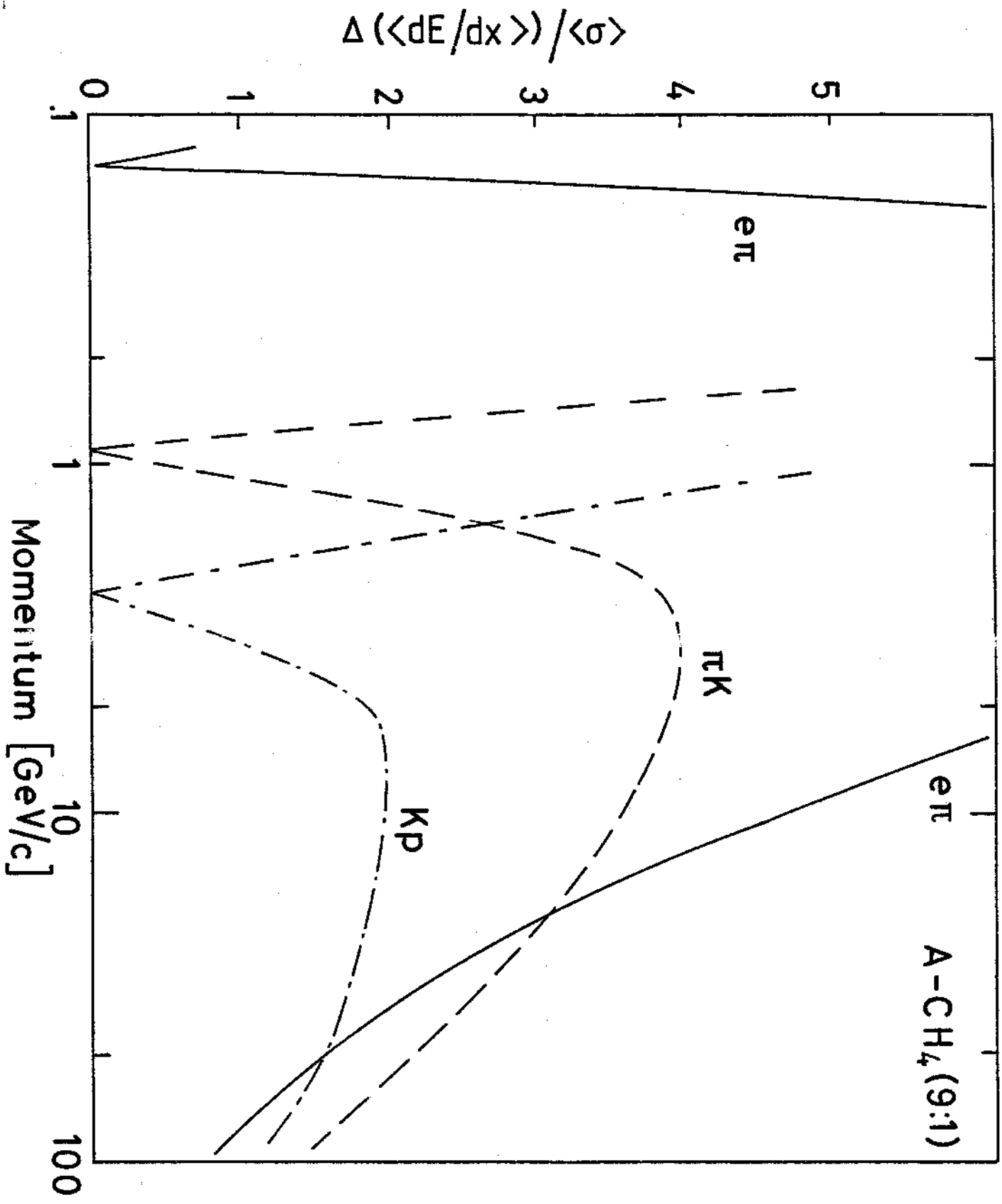


FIG. 2b  
 Particle separation  
 in units of the  
 resolution based on  
 $(\sigma) = 3.5\% \cdot \frac{dE}{dx}$

2 400

9 900

- (A) SUPERCONDUCTING SOLENOID
- (B) CRYOSTAT
- (C) YOKE BARREL
- (D) YOKE END-CAP
- (E) COMPENSATING COIL
- (F) SOLENOID SUPPORT STRUCTURE
- (G) MOBILE PLATFORM

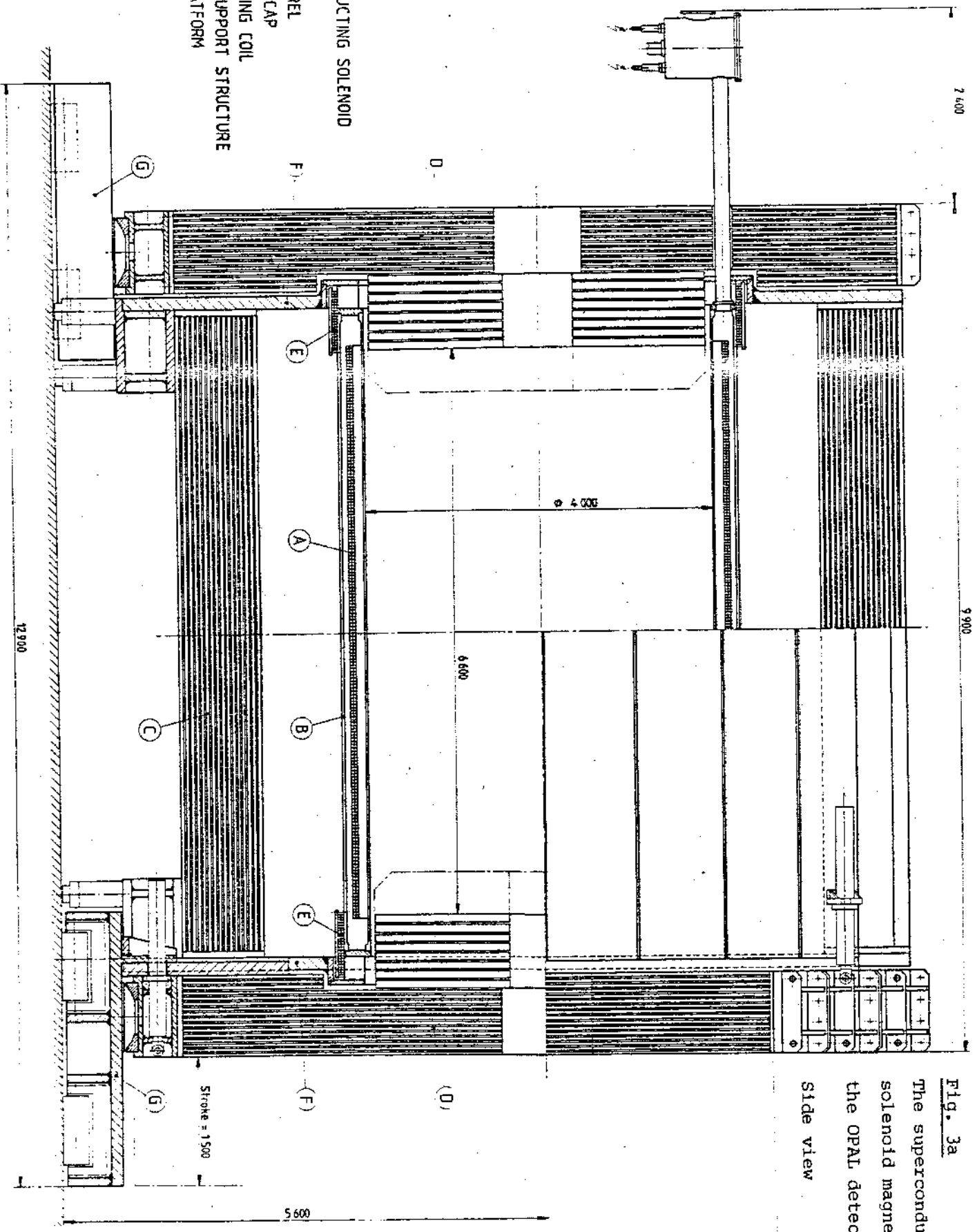


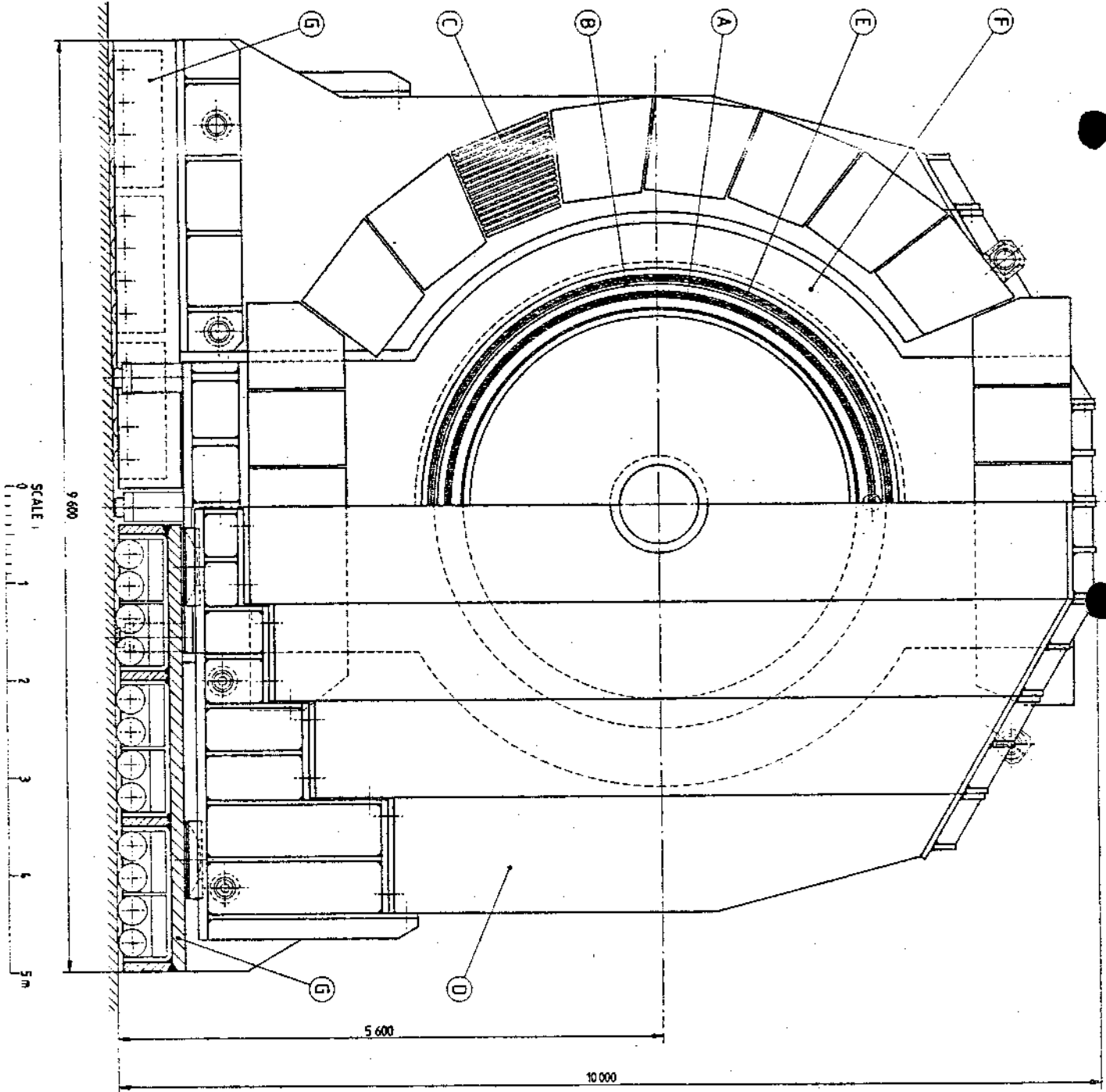
Fig. 3a

The superconducting solenoid magnet for the OPAL detector  
Side view

Fig. 3b  
 The superconducting  
 solenoid magnet for  
 OPAL detector

End view

- Ⓐ SUPERCONDUCTING SOLENOID
- Ⓑ CRYOSTAT
- Ⓒ YOKE BARREL
- Ⓓ YOKE END-CAP
- Ⓔ COMPENSATING COIL
- Ⓕ SOLENOID SUPPORT STRUCTURE
- Ⓖ MOBILE PLATFORM





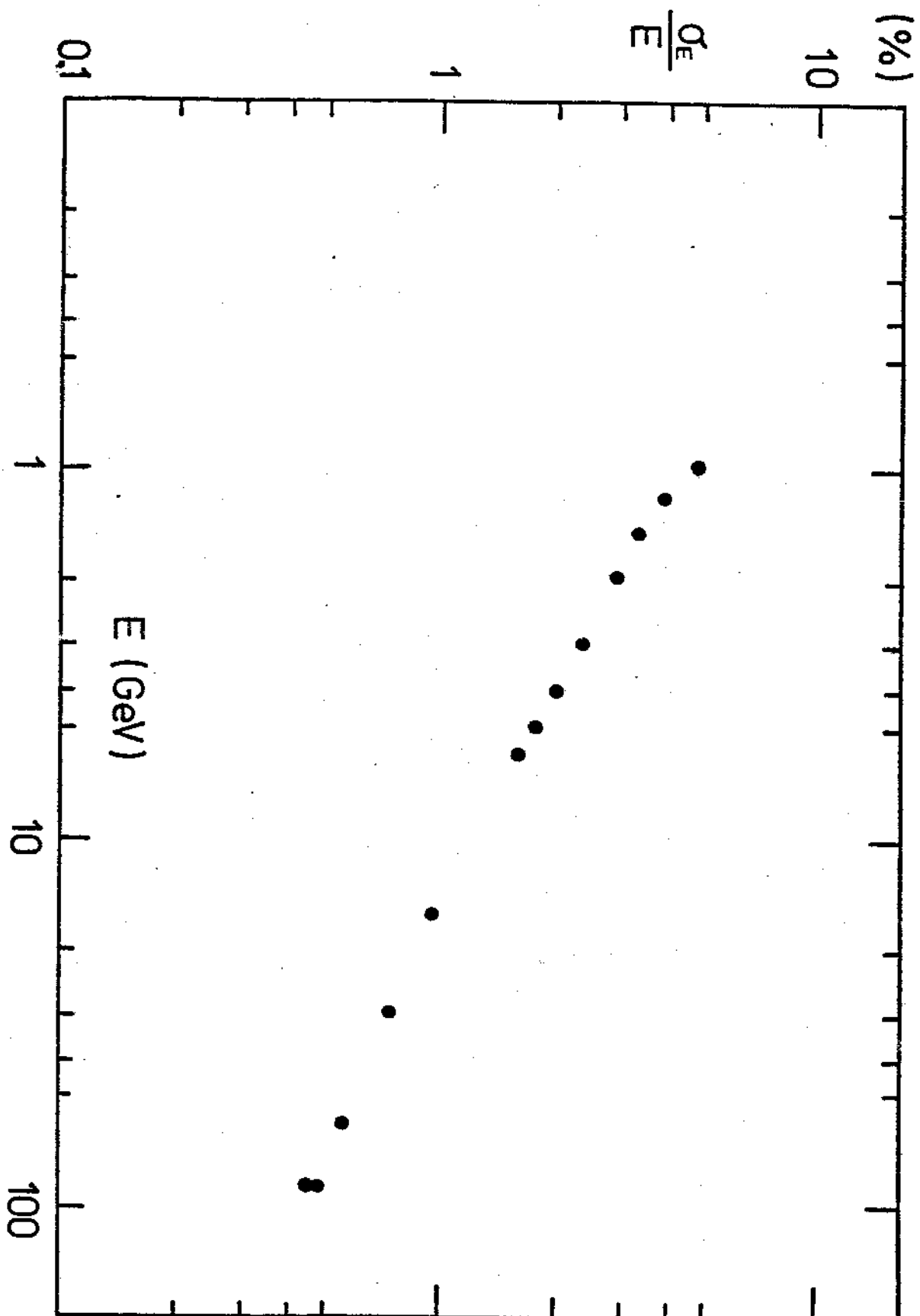


Fig. 4a: Energy resolution of the lead glass shower counters as a function of electron energy

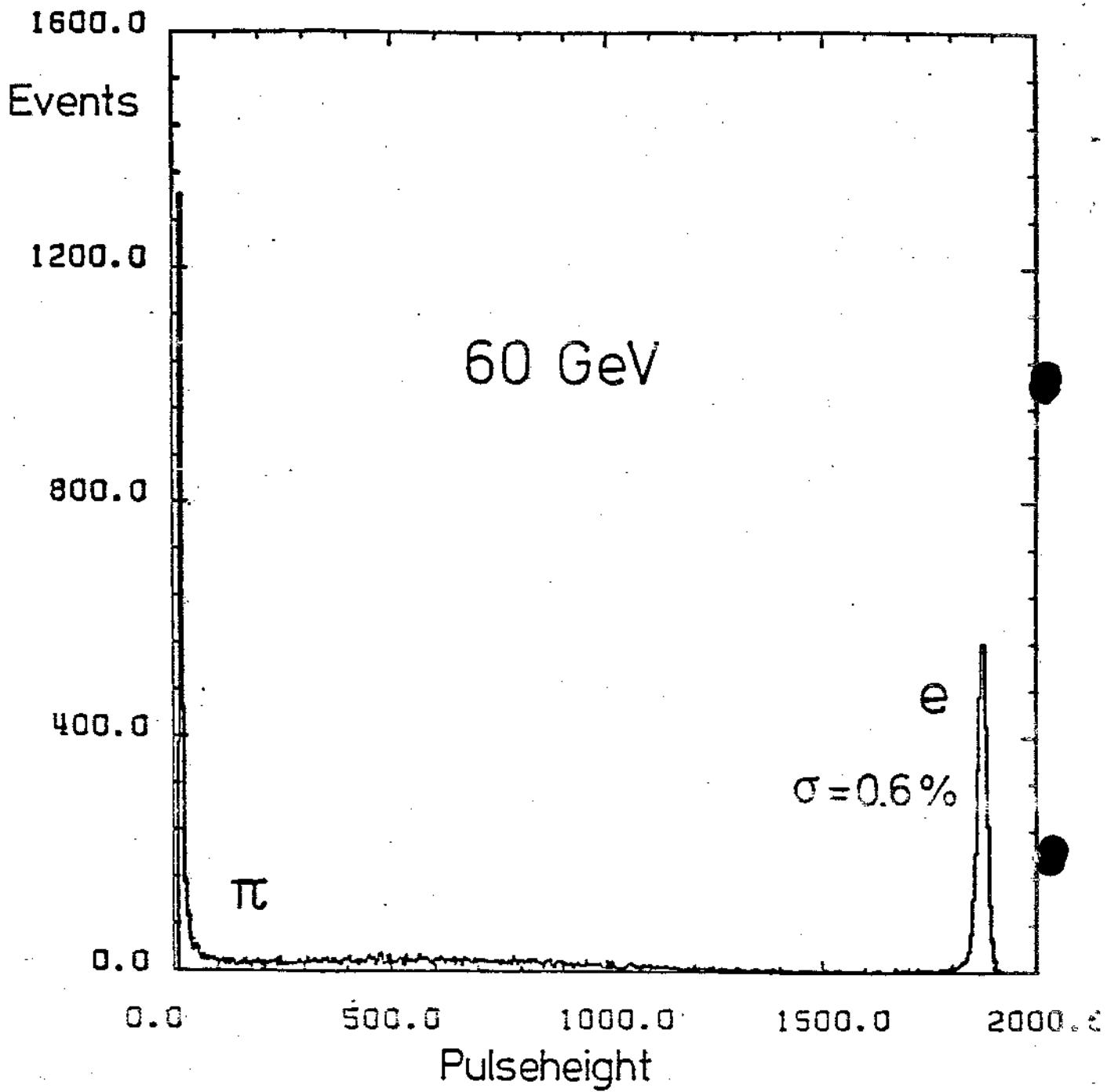


Fig. 4b: Pulseheight spectrum of leadglass counters  
for 60 GeV/c electrons and pions